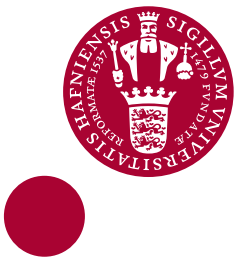

r-PROCESS CALCULATIONS WITH A MICROSCOPIC DESCRIPTION OF THE FISSION PROCESS

Giuliani, S. A.; Martinez-Pinedo, G.; Robledo, L. M.; Wu, M. -R.

Published in:
Acta Physica Polonica B

DOI:
10.5506/APhysPolB.48.299

Publication date:
2017

Document version
Publisher's PDF, also known as Version of record

r-PROCESS CALCULATIONS WITH A MICROSCOPIC DESCRIPTION OF THE FISSION PROCESS*

S.A. Giuliani[a], G. Martínez-Pinedo[a], L.M. Robledo[b], M.-R. Wu[a,c]

[a]Institut für Kernphysik (Theoriezentrum), Technische Universität Darmstadt
Schlossgartenstraße 2, 64289 Darmstadt, Germany
[b]Departamento de Física Teórica, Universidad Autónoma de Madrid
28049 Madrid, Spain
[c]Niels Bohr International Academy, Niels Bohr Institute
Blegdamsvej 17, 2100 Copenhagen, Denmark

(Received December 14, 2016)

We computed the fission properties of nuclei in the range of $84 \leq Z \leq 120$ and $118 \leq N \leq 250$ using the Barcelona–Catania–Paris–Madrid (BCPM) Energy Density Functional (EDF). For the first time, a set of spontaneous and neutron-induced fission rates were obtained from a microscopic calculation of nuclear collective inertias. These fission rates were used as a nuclear input in the estimation of nucleosynthesis yields on neutron star mergers. We founded that the increased stability against the fission process predicted by the BCPM allows the formation of nuclei up to $A = 286$. This constitutes a first step in a systematic exploration of different sets of fission rates on r-process abundance predictions.

DOI:10.5506/APhysPolB.48.299

1. Introduction

The rapid neutron capture process (r-process) is responsible for the production of half of the elements heavier than iron that are observed in stars of different metallicities as well as in the solar system. The quest to identify its actual astrophysical site is still ongoing, but there are strong indications that make neutron star mergers (NSM) a likely candidate. Realistic r-process calculations for matter ejected in NSM require the knowledge of nuclear properties and decay modes of nuclei covering the region from the valley of stability to the neutron drip-line. The major challenge comes from the fact that most of the nuclei involved in r-process calculations cannot be

* Presented at the Zakopane Conference on Nuclear Physics "Extremes of the Nuclear Landscape", Zakopane, Poland, August 28–September 4, 2016.

measured at the laboratories and their nuclear properties must be extracted from theoretical models bringing a large uncertainty in the final predictions of the nucleosynthesis yields [1–3]. In this work, we will focus on the role played by fission using a consistent and microscopic calculation of both the potential energy surfaces and the collective inertias within the framework of the Self-Consistent Mean-Field (SCMF) theory with EDFs [4].

2. Role of fission

Following the Hartree–Fock–Bogoliubov (HFB) theory with constraining operators, we computed the fission properties of nuclei in the region of $84 \leq Z \leq 120$ and $118 \leq N \leq 250$ using the BCPM EDF [5]. The probability of the nucleus to penetrate the fission barrier and undergo fission is given, within the semiclassical Wentzel–Kramers–Brillouin (WKB) approach, by the action integral computed along the fission path

$$S = \int \mathrm{d}Q_{20} \sqrt{2\mathcal{M}(Q_{20})\,[\mathcal{V}(Q_{20}) - E_0]}\,, \tag{1}$$

being $\mathcal{M}$, $\mathcal{V}$ and E_0 the collective inertia, effective potential energy and collective ground-state energy of the nucleus. The only collective degree of freedom describing the evolution of the potential energy surface is the axial quadrupole moment operator $Q_{20} = z^2 - \frac{1}{2}(x^2 + y^2)$ representing the axially symmetric stretching of the nucleus (see [6, 7] for further details). Collective inertias are calculated within the Adiabatic Time-Dependent HFB (ATDHFB) scheme and bulk properties of nuclei with an odd number of protons and/or neutrons are obtained using the Perturbative Nucleon Addition Method (PNAM) [8].

In r-process calculations, the most relevant fission decay mode is the neutron-induced fission process, where the penetration probability is computed using Eq. (1) and replacing the collective ground state energy E_0 by the excitation energy of the compound nucleus after the neutron capture. In a first approximation, one can compute this excitation energy as the neutron separation energy of the parental nucleus and, therefore, the competition between the neutron capture and the neutron-induced fission is given by the difference between the neutron separation energy S_n and the fission barrier B_f. The BCPM prediction of this neutron-induced "energy window" is shown in the upper panel of Fig. 1. A simple estimation of the r-process path, given by nuclei with a constant neutron separation energy of 2 MeV [9], is depicted with a solid line. For nuclei with $Z \leq 92$, the r-process path proceeds through a region where the neutron induced fission is highly suppressed, with values of $B_\mathrm{f} - S_n \gtrsim 10$ MeV. But once the predicted neutron magic number $N = 184$ is reached, the r-process path moves

towards a region of lower fission barriers where the neutron-induced fission starts to compete with neutron capture. This competition between neutron capture and neutron-induced fission for nuclei around $Z/N = 102/188$ is reflected in the lower panel of Fig. 1 showing the dominating decay channel of each nucleus. Nuclei beyond the neutron drip-line were excluded from the plot since they are expected to decay back to stability by neutron emission. In this plot, we see that BCPM calculations predict a corridor between the r-path and the neutron drip-line where the neutron capture dominates up to nuclei with mass number $A = 340$. In the next section, we will show that this corridor allows for the production of the heaviest nuclei when the neutron-capture freezes out. Finally, from Fig. 1, it is possible to conclude that the spontaneous fission decay plays a relevant role in r-process calculations only in the region of nuclei with $B_{\mathrm{f}} \leq 2$ MeV.

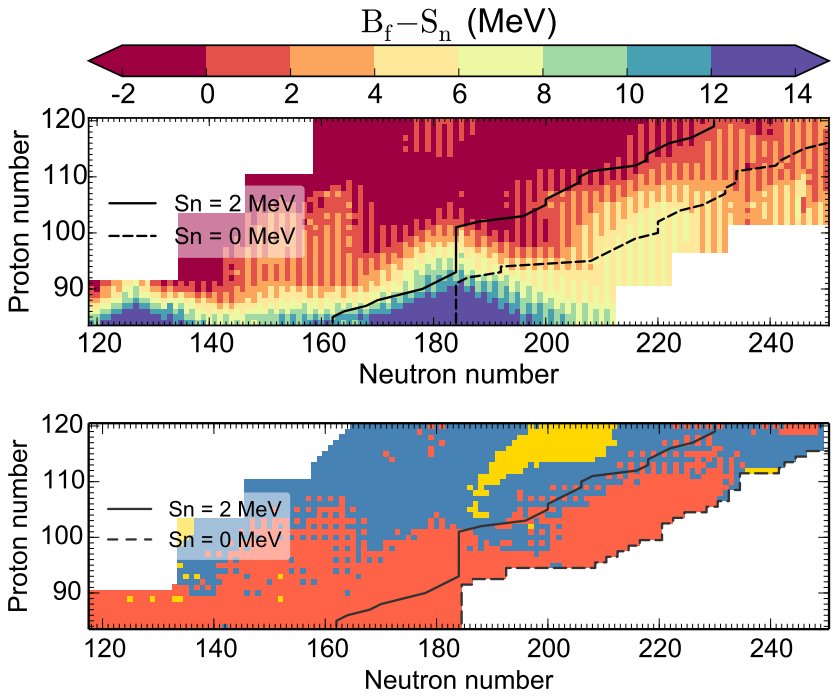

Fig. 1. The neutron-induced energy window given as $B_{\mathrm{f}} - S_n$ in MeV (upper panel) and dominating decay channel (lower panel) predicted by the BCPM EDF. Dashed line represents the neutron drip-line. As an hint of the r-process path, the heaviest isotope of each specie with $S_n \gtrsim 2$ MeV are connected by a solid line.

3. r-process nucleosynthesis calculations

Using the nuclear inputs provided by the BCPM interaction, we computed the neutron-induced rates relevant for r-process nucleosynthesis for nuclei with $Z \geq 84$. For the first time, a complete set of neutron-induced fission rates was obtained from microscopic calculations of the collective inertias using the TALYS nuclear reaction code[1]. All rates were calculated using the Back-shifted Fermi gas model for level densities and the Kopecky–Uhl generalized Lorentzian gamma-ray strength functions. The new set of neutron capture, photodissociation, spontaneous and neutron-induced fission rates was used for running r-process calculations for a single standard trajectory simulating the dynamic ejecta in neutron star mergers [2]. When experimental data was not available, masses of nuclei with $Z < 84$ were adopted from the Finite Range Droplet Model (FRDM), mass model [11] and β-decay rates from the compilation of Möller *et al.* [12]. Figure 2 shows the abundances obtained in our calculations at three different phases of the evolution: when the neutron-to-seed ratio becomes equal to one, marking the beginning of the neutron-capture freeze out (right panel); the time when the beta-decay rate equals the neutron-capture rate and the material starts to decay back to stability (middle panel); and at 1 Gy, when most of the material left can be considered stable. The abundances of this work are compared with previous calculations [2] obtained from the astrophysical reaction rates of Panov *et al.* [10] based on the FRDM mass model and the

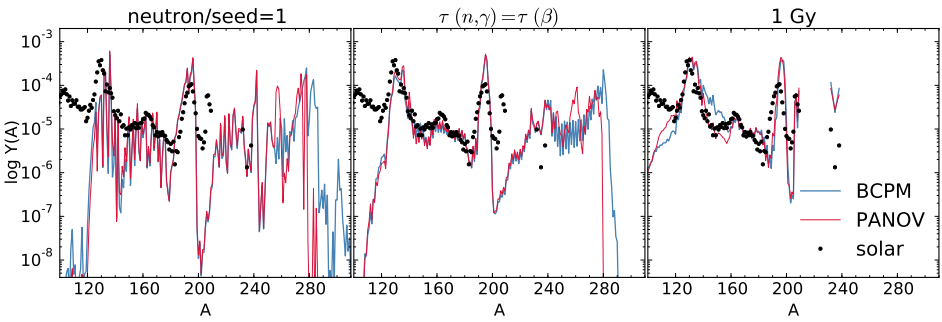

Fig. 2. r-process abundances from matter dynamically ejected in NSM for two different sets of neutron-induced stellar rates: BCPM (this work, thick line) and Panov *et al.* [10] (thin line). The three panels show different phases of the evolution: when the neutron-to-seed ratio becomes equal to one (right panel); the time when the beta-decay rate equals the neutron-capture rate (middle panel); and at 1 Gy, when most of the material has decayed back to stability. Bullets represent the solar r-process relative abundances.

[1] `http://www.talys.eu/`

Thomas–Fermi (TF) fission barriers [13]. The fission barriers predicted by the TF model for nuclei around the r-path are, in general, 2 MeV lower than those predicted by BCPM for the same nuclei. One consequence of the higher barriers predicted by BCPM is the larger production of material with $283 \leq A \leq 286$ at the early stages of the evolution, as it is shown in the right and middle panel of Fig. 2. This material is produced by nuclei accumulated above the (predicted) magic neutron number $N = 184$ (see Fig. 3), where $B_{\rm f} \sim 8$ MeV. Some of these nuclei will afterward decay by spontaneous fission, increasing the yields above the second peak ($120 \leq A \leq 160$) as it is shown in the right panel of Fig. 2. In Fig. 3, we can see that nuclei with a mass number up to 320 can be produced at the neutron freeze-out in the corridor described in Sec. 2. However, a larger production of such heavy nuclei is prevented by the low neutron separation energies of nuclei in this region and the fact that the r-path has to overcome a rather broad region of nuclei around $Z/N = 100/190$, where the neutron-induced fission decay dominates over neutron capture (see lower panel in Fig. 1). Comparing our results with previous r-process calculations of Petermann *et al.* [14], we found that our abundances at the freeze out resembles those obtained using the Extended Thomas–Fermi Model with Strutinski Integral (ETSFI) nuclear masses and fission barriers.

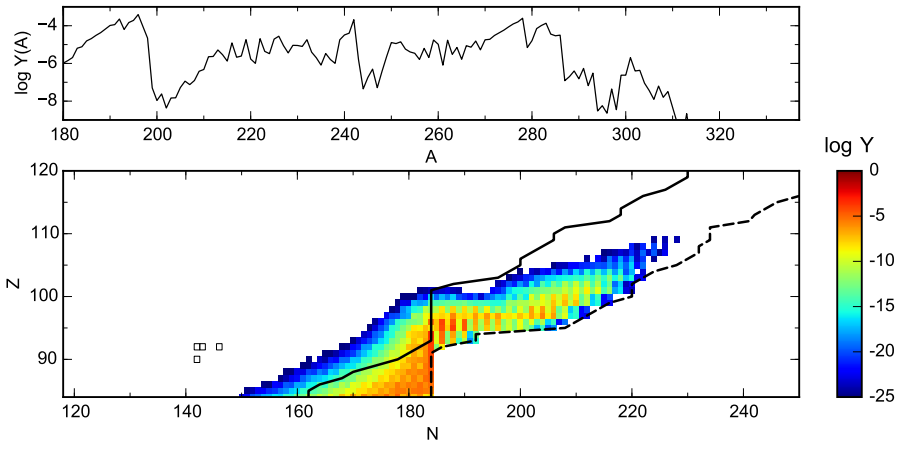

Fig. 3. r-process abundances at the neutron freeze-out (ratio of neutrons to seed nuclei equals to 1) as a function of the mass number A (upper plot) and as a contour plot (lower plot). Empty boxes in the lower plot represent stable nuclei.

4. Conclusions

We presented the r-process abundances for matter ejected dynamically in neutron star mergers using the BCPM fission properties. The neutron-induced fission rates obtained in this study allow the production of r-process nuclei up to $A = 310$, and compared to previous calculations [2] increase the amount of material accumulated around $A = 285$. In order to fully understand the impact of a microscopic calculations of fission rates in r-process nucleosynthesis, a consistent computation of beta-delayed fission rates and the comparison with results coming from other EDFs is required. Work in this direction is already in progress.

S.A.G., G.M.P. and M.-R.W. acknowledge support from the Helmholtz Association through the Nuclear Astrophysics Virtual Institute (VH-VI-417), and the BMBF-Verbundforschungsprojekt number 05P15RDFN1. M.-R.W. acknowledges support from the Villum Foundation (Project No. 13164) and the Danish National Research Foundation (DNRF91). The work of L.M.R. was supported in part by the Spanish Ministerio de Economía y Competitividad (MINECO), under contracts Nos. FIS2012-34479, FPA2015-65929, FIS2015-63770 and by the Consolider-Ingenio 2010 Program MULTIDARK.

REFERENCES

[1] S. Goriely, *Eur. Phys. J. A* **51**, 22 (2015).
[2] J.J. Mendoza-Temis *et al.*, *Phys. Rev. C* **92**, 055805 (2015).
[3] D. Martin *et al.*, *Phys. Rev. Lett.* **116**, 121101 (2016).
[4] M. Bender, P.-H. Heenen, P.-G. Reinhard, *Rev. Mod. Phys.* **75**, 121 (2003).
[5] M. Baldo *et al.*, *Phys. Rev. C* **87**, 064305 (2013).
[6] S.A. Giuliani, L.M. Robledo, *Phys. Rev. C* **88**, 054325 (2013).
[7] S.A. Giuliani, G. Martínez-Pinedo, L.M. Robledo, in preparation.
[8] T. Duguet *et al.*, *Phys. Rev. C* **65**, 014310 (2001).
[9] G. Martínez-Pinedo, *Eur. Phys. J. Spec. Top.* **156**, 123 (2008).
[10] I.V. Panov *et al.*, *Astron. Astrophys.* **513**, A61 (2010).
[11] P. Möller *et al.*, *At. Data Nucl. Data Tables* **59**, 185 (1995).
[12] P. Möller, B. Pfeiffer, K.-L. Kratz, *Phys. Rev. C* **67**, 55802 (2003).
[13] W.D. Myers, W.J. Swiatecki, *Phys. Rev. C* **60**, 14606 (1999).
[14] I. Petermann *et al.*, *Eur. Phys. J. A* **48**, 122 (2012).